Supplementary experimental procedures

Animals and treatments

C57BL/6 WT, RORγt$^{-/-}$, SK1$^{-/-}$ and SK2$^{-/-}$ mice were obtained from Jackson Laboratory. All animal procedures were approved by the University of Louisville Institutional Animal Care and Use Committee. We used the binge-on-chronic NIAAA (Gao) model with 8-week-old mice. Briefly, male or female mice were acclimated to the Lieber-DeCarli liquid control diet (F1259SP; Bio-Serv, Flemington, NJ) or gradually introduced to and increased on the ethanol diet (5% ethanol-w/v; F1258SP; Bio-Serv) for 5 days followed by further feeding with the liquid control (pair feeding, PF) or ethanol diet (alcohol feeding, AF) for additional 10 days (day 15), 17 days (day 22), or 23 days (day 28). On the last day of feeding, mice were also given ethanol 5 g/kg or maltose dextran 9 g/kg by gavage, and sacrificed 8 hours later. The volume of control diet given to mice was matched to the volume of ethanol diet consumed. Because 5-ASA at 100 mg/kg was the concentration of 5-ASA closest to that used to treat IBD in humans (1, 2), we selected 50 and 100 mg/kg as the optimal concentration of 5-ASA for the study in AF mice. 5-ASA (50 mg/kg/d) was administered orally for 5 days before feeding the Lieber-DeCarli liquid diet, and then administered orally once daily until the end of experiment. The anti-inflammatory effects of 5-ASA were evaluated by administration of different dosages (50 mg/kg/d-1,000 mg/kg/d). For SKI-178 treatment, mice were treated with SKI-178 (5 mg/kg) i.v. every 48 hours until the end of experiment (day15). In some experiments, mice were given FTY720 (1 mg/kg) orally daily with/without 5-ASA during ethanol feeding.

Reagents, antibodies and flow cytometry

FTY720, ALT, AST and ALP assay Kits were purchased from Thermo Fisher Scientific. SK1-178 was purchased from Sigma-Aldrich. Rat anti-mouse-IL-17A (17F3) was purchased from BioXcell (West Lebanon, New Hampshire). For analysis of surface markers, cells were stained in PBS containing 2% (wt/vol) BSA. Intracellular staining of the transcription factors Foxp3 was performed using the Foxp3 Fix/Perm Buffer Set (eBioscience, Thermo fisher). For detection of intracellular cytokines, cells were first stimulated for 4 h with 50 ng/ml PMA and 1µg/ml ionomycin in the presence of Brefeldin A (5µg/ml; All obtained from Sigma), followed by staining for surface markers. Cells were then fixed and permeabilized using the Foxp3 Fix/Perm Buffer Set and stained for intracellular cytokines. The following antibodies were used at a dilution of 1/200–1/600: PerCP-Cy5.5, PE-, FITC- or APC-labeled anti-IL-17A (TC11–18H10.1), PE- or APC-labeled anti-IL-4 (11B11, eBioscience, Thermo fisher), PE- or APC-labelled anti-IL-10 (JES5–16E3), APC- or PE-Cy7-labeled anti-IFN (XMG1.2), PE-labeled anti-Foxp3 (FJK-16s, eBioscience, Thermo fisher), PE-, FITC- or APC-labeled anti-CD11b (M1/70), PE-, FITC- or APC-labeled anti-CD4 (RM4-5), PE-Cy7-labeled anti-CD3 (145-2C11), PE-anti-Gr-1 (RB6-8C5), PE- or FITC-labeled anti-mouse Ly6G (1A8), APC-conjugated CD45.2 (104), PE-conjugated anti-CD45.1 (A20), FITC-, PerCP-Cy5.5 or Pacific Blue-labelled anti-CD45 (30-F11), PE-anti-SCA1 (D7), PE-anti-S1PR1 (FAB7089P,R&D). All antibodies were obtained from ThermoFisher unless otherwise noted. Flow cytometry data were acquired on a 5-color FACScan (Becton Dickinson) and analyzed using FlowJo software (Treestar). Cell sorting was performed using a FACSAria II.

Histology and immunohistochemistry

Tissue specimens were fixed in 10% formalin, dehydrated, and then embedded in paraffin. Tissue samples were cut at 5 µm thicknesses and stained with hematoxylin and eosin. For immunofluorescence analysis, tissue sections were subjected to antigen retrieval by boiling the slides in Antigen Unmasking Solution (Vector Laboratories) for 10 minutes according to instructions. Sections were then blocked for 1 hour at 22°C with 5% BSA in PBS and incubated overnight at 4°C with the primary antibodies, i.e., rabbit polyclonal MUC2 and phospho-Stat3^{Tyr705} antibody from Cell Signaling used at a dilution of 1/250, mouse monoclonal anti-MUC2, anti-SK1 and lysozyme were purchased from Abcam (Cambridge, United Kingdom) and used at a dilution of 1/200. Primary antibodies were detected by Alexa Fluor 488, 594 or 647 conjugated goat anti-mouse, anti-rabbit IgG and anti-rat (1:600, Invitrogen). Tissues were counterstained with DAPI and images were captured on a Zeiss LSM 510 confocal microscope equipped with a digital image analysis system (Pixera). For immunohistochemistry analysis of myeloperoxidase (MPO)-positive neutrophils or macrophages, OCT (Sakura Finetek)-embedded tissue cryosections (9µm-thick) were stained with MPO or F4/80 (BM8, ebioscience, ThermoFisher), followed by staining with horseradish peroxidase-conjugated anti-IgG second antibodies. Antigens were then visualized with 3,3′-diaminobenzidine substrate (Vector Laboratories) and scanned using an Aperio Imagescope. Intestinal Goblet cells were evaluated by Alcian Blue staining. Hepatic collagen was detected by Picro Sirius Red Staining.

For Oil Red O staining, frozen sections were incubated with 60% isopropanol for 1 minute. Tissues were dried in a 37°C incubator for approximately 10 minutes before incubating with Oil Red O solution. Slides were incubated with Oil Red O solution for 15

minutes. The Oil Red O solution was aspirated from the slides, and 60% isopropanol was added to the slides for several minutes to remove any residual Oil Red O. The slides were washed in PBS and stained for 30 seconds with hematoxylin (GHS132; Sigma,) followed by more washes in dH_2O. Coverslips were mounted on slides with a mounting medium (glycerol in PBS 6:1) followed by microscopy.

Measurement of Liver TGs

Hepatic TG extraction was performed as described previously(3). Briefly, approximately 20-50 mg of liver tissue was ground into powder and incubated in 1 mL of a chloroform-methanol (2:1) mixture for 1 hour with vigorous shaking. ddH2O (200 µL) was added to the samples, and the samples were vortexed and centrifuged at 3,000*g* for 5 minutes to separate out the lipid phase. The lower lipid phase was collected and dried, and the remaining pellet was dissolved in a *tert*-butanol, Triton X-114, and methanol (9:4:2) mixture. Triglyceride content was determined using commercially available colorimetric kits (Thermo Fisher, Waltham, MA). Tissue triglyceride Liver tissues were homogenized in distilled water and the homogenate was collected for lipid extraction.

Gut Permeability Assays

We performed gut permeability assays by orally gavaging overnight-fasted mice with 0.5-1 mg/g body weight of FITC-conjugated dextran (Sigma) and collecting plasma after 3 hr. We prepared standards and measured fluorescence at 485/528 nm as previously described(4).

Serum ALT and lipid profile assay

Mouse serum was collected by orbital vein bleeding at the time of euthanasia. Serum alanine aminotransferase (ALT) and AST were analyzed using the Piccolo Xpress system (ABAXIS, Union City, CA) or Kits from Thermo Fisher Scientific.

Human Samples

Paraffin-embedded liver sections and cryo-liver tissues from healthy liver donors (n = 6) and patients with AH (n = 6) were obtained from John Hopkins University (Dr.Zhaoli Sun). The detail demographic, clinical, and biological characterization information of the patients and health controls was recently described by Khanova et al(5). Serum from patients with moderate AH (n=13) and severe AH (n=13) were obtained from University of Louisville Hospital and all patients signed Informed Consent documents prior to entering the study. Supplemental Table 1 included demographics, drinking history, and clinical markers in patients with severe acute alcoholic hepatitis (AAH), moderate AAH, and healthy controls.

RNA extraction and PCR

Total RNA was isolated from the tissue or lymphocytes of MLNs, small intestine and colon using the Qiagen RNeasy RNA isolation Kit and was used to synthesize cDNA. RNA (1μg) was reverse-transcribed with Superscript III and random primers (Invitrogen). For quantitation of genes of interest, cDNA samples were amplified in applied biosystems Realtime System using SYBR Green Master Mix (Invitrogen) and specific primers (Supplemental Table 2) according to the manufacturer's instructions. Fold changes in mRNA expression between treatments and controls were determined by the δCT method as described(6). Results for each sample were normalized to the concentration of GAPDH mRNA measured in the same samples and expressed as fold increase over baseline

levels, which are set at a value of 1. Differences between groups were determined using a two-sided Student's *t*-test and one-way ANOVA. Error bars on plots represent ± SEM, unless otherwise noted. All primers were purchased from Eurofins MWG Operon.

ELISA

The quantity of IL-17A, IL-6, TNF-α, IL-10, IFN-γ (Thermo Fisher, eBioscience) were determined in culture supernatants, serum and tissue using ELISA kits according to the manufacturer's instructions. The sensitivity of the assay was <20 pg/ml.

Western blot analysis

Tissue or cells were disrupted in lysis buffer containing 1% Triton X-100, 0.1% SDS, 150 mM NaCl, 50 mM Tris-HCl, 1 mM EDTA, 1 mM EGTA, 5 mM sodium molybdate and 20 mM phenylphosphate with protease and phosphatase inhibitors (1 mM PMSF, 10 μg ml^{-1} aprotinin, 20 μg ml^{-1} leupeptin, 20 μg ml^{-1} pepstatin A, 50 mM NaF and 1 mM sodium orthovanadate) for 30 min on ice. The samples were centrifuged (16,000*g*, 10 min, 4°C) and the resulting supernatants transferred to fresh tubes. Protein lysates were quantitated using a Bio-Rad protein kit (Bio-Rad) and 50-100 μg of lysates were separated on 10% SDS polyacrylamide gels and transferred to a nitrocellulose membrane. Rabbit anti-phospho-Stat3 (727), phospho-Stat3 (Tyr705), STAT3 and actin were purchased from Cell Signaling Technology (Danvers, MA) and used at a dilution of 1/1,000. Membranes were probed with specific antibodies and protein quantity visualized using the ChemiDoc Imaging Systems (Bio-Rad, Hercules, California). Images have been cropped for presentation.

Isolation of lamina propria lymphocytes (LPLs) and hepatic immune cells

The method used for isolation of LPLs has been previously described(7). In brief, fat tissues and Peyer's patches (PPs) were removed from small intestine. The intestine was

open and cut in pieces 1-cm long and incubated in an HBSS solution containing 5 mM EDTA and 10 mM Hepes for 30 min at 37°C with slow rotation (180 r.p.m.). Pieces were then cut into smaller pieces and incubated in an HBSS solution containing 0.5 mg ml^{-1} DNase I (Roche) and 1 mg ml^{-1} collagenase type IV (Worthington). Finally, the solution containing digested tissue was passed through a 100-µm cell strainer and LPLs were recovered at the interface of the 40 and 72% Percoll (GE Healthcare) solutions. Livers were perfused with saline solution by way of the portal vein which was followed by enzymatic digestion. Liver immune cells were purified by centrifugation using a Percoll gradient as described previously. For flow cytometry analysis, the cells were labelled using standard procedures described above.

Sphingolipid analysis

Ceramide species, sphingosine and S1P from gut and liver of mice and human serum were collected and analyzed with LC-MS/MS by the Lipidomics/Metabolomics Shared Resource (Virginia Commonwealth University), as previously described[7]. In brief, calibration curves were constructed by plotting peak area ratios of synthetic standards corresponding to each target analyte with respect to the appropriate internal standard. The target analyte peak areas from the samples were similarly normalized to their respective internal standard and then compared with the calibration curves using a linear regression model. Results were normalized to total protein levels. In some experiments, S1P were also analyzed by HPLC(7).

Statistical Analysis

Values are shown as Mean $\pm$ SEM except where otherwise indicated. Comparison of multiple experimental groups was performed by two-way ANOVA with appropriate

multiple comparison tests. A t test was used to compare the means of two groups. The p values < 0.05 were considered to be statistically significant. Sample sizes are calculated to allow significance to be reached.

Table 1: Demographics, drinking history, and clinical markers in patients with severe acute alcoholic hepatitis (AH), moderate AH, and healthy controls. Data are presented as Mean ± SD (standard deviation).

	Severe AH (n=13)	**Moderate AH (n=13)**	**Healthy Control (n=11)**
Sex (Female, %)	5 (38.4%)	2 (15.38%)	6 (54.55%)
Age (yrs.)	49.2±7.96	51.05±8.19	32.46±10.65
Weight (lb.)	206.64±67.62	235.14±38.59	159.56±28.46
AUDIT	20.67±8.53	22.31±9.87	NA
MELD	29.23±8.88	14.84±3.29	NA
Maddrey	82.62±60.19	31.83±26.99	NA
Total Bilirubin (mg/dl)	18.28±11.23	5.1±5.42	0.68±0.27
Albumin (g/dL)	2.36±0.69	3.06±0.92	4.1±0.28
AST (U/L)	225.77±364.03	138.92±98.49	28.56±14.45
ALT (U/L)	67.92±68.21	77.92±55.42	29.89±30.03
AST:ALT	2.88±0.94	1.95±1.22	1.16±0.28
Creatinine (mg/dL)	1.34±0.75	0.95±0.39	0.88±0.14
ALP (U/L)	146.46±87.81	161.46±91.19	51.00±10.60
INR	2.55±1.23	1.40±0.49	NA
CPT	11.15±0.80	8.38±2.06	NA
Lille Score	0.58±0.27	0.13±0.08	NA

Supplemental table 2. Primers used for Real-time PCR

Gene name	Forward primer	Reverse primer
GAPDH	AGGTCATCCCAGAGCTGAACG	ACCCTGTTGCTGTAGCCGTAT
β-Actin	ACGGCCAGGTCATCACTATTC	AGGAAGGCTGGAAAAGAGCC
TNF-α	TCTATGGCCCAGACCCTCAC	GACGGCAGAGAGGAGGTTGA
MMP9	AATCTCTTCTAG AGACTG GGAAGGAG	AGC TGA TTG ACT AAA GTA GCT GGA
SK2	CCACCTGAGCTCCGAGCTGTT	GGCACATGAACCAGGTATGGA
SK1	GAGCTCCGAGCTGTTTGCA	TGACACCCCCGCACGTA
RORA	GAACACCTTGCCCAGAACAT	AGCTGCCACATCACCTCTCT
S1PR1	GTGTAGACCCAGAGTCCTGCG	AGCTTTTCCTTGGCTGGAGAG
IL-17A	TTTAACTCCCTTGGCGCAAAA	CTTTCCCTCCGCATTGACAC
COX2	TGAGTACCGCAAACGCTTCT	CTCCCCAAAGATAGCATCTGG
RORC	GACCCACACCTCACAAATTGA	AGTAGGCCACATTACACTGCT
IFN-γ	TCAGCAACAGCAAGGCGAAAAAGG	CCACCCCGAATCAGCAGCGA
ZO1	TGGGAACAGCACACAGTGAC	GCTGGCCCTCCTTTTAACAC
IL-6	GAGAGGAGACTTCACAGAGGATAC	GTACTCCAGAAGACCAGAGG
MUC2	AGGGCTCGGAACTCCAGAAA	CCAGGGAATCGGTAGACATCG
OCCLN	ACCCGAAGAAAGATGGATCG	CATAGTCAGATGGGGGTGGA
Muc5a	GTGGTTTGACACTGACTTCCC	CTCCTCTCGGTGACAGAGTCT
S100A8	ACAATGCCGTCTGAACTGG	CTCTGCTACTCCTTGTGGCTGTCT
S100A9	GGAGCGCAGCATAACCAC	GCCATTGAGTAAGCCATTCC
MUC5b	GTGGCCTTGCTCATGGTGT	GGACGAAGGTGACATGCCT

1. Rousseaux C, Lefebvre B, Dubuquoy L, Lefebvre P, Romano O, Auwerx J, Metzger D, et al. Intestinal antiinflammatory effect of 5-aminosalicylic acid is dependent on peroxisome proliferator-activated receptor-gamma. Journal of Experimental Medicine 2005;201:1205-1215.
2. Brown JB, Lee G, Managlia E, Grimm GR, Dirisina R, Goretsky T, Cheresh P, et al. Mesalamine inhibits epithelial beta-catenin activation in chronic ulcerative colitis. Gastroenterology 2010;138:595-605, 605 e591-593.
3. Shao T, Zhao C, Li F, Gu Z, Liu L, Zhang L, Wang Y, et al. Intestinal HIF-1alpha deletion exacerbates alcoholic liver disease by inducing intestinal dysbiosis and barrier dysfunction. J Hepatol 2018;69:886-895.
4. Dong CX, Zhao W, Solomon C, Rowland KJ, Ackerley C, Robine S, Holzenberger M, et al. The intestinal epithelial insulin-like growth factor-1 receptor links glucagon-like peptide-2 action to gut barrier function. Endocrinology 2014;155:370-379.
5. Khanova E, Wu R, Wang W, Yan R, Chen Y, French SW, Llorente C, et al. Pyroptosis by caspase11/4-gasdermin-D pathway in alcoholic hepatitis in mice and patients. Hepatology 2018;67:1737-1753.
6. Xiang Y, Ma N, Wang D, Zhang Y, Zhou J, Wu G, Zhao R, et al. MiR-152 and miR-185 co-contribute to ovarian cancer cells cisplatin sensitivity by targeting DNMT1 directly: a novel epigenetic therapy independent of decitabine. Oncogene 2014;33:378-386.
7. Deng ZB, Mu JY, Tseng M, Wattenberg B, Zhuang XY, Egilmez NK, Wang QL, et al. Enterobacteria-secreted particles induce production of exosome-like S1P-containing particles by intestinal epithelium to drive Th17-mediated tumorigenesis. Nature Communications 2015;6.

Supplementary Figures:

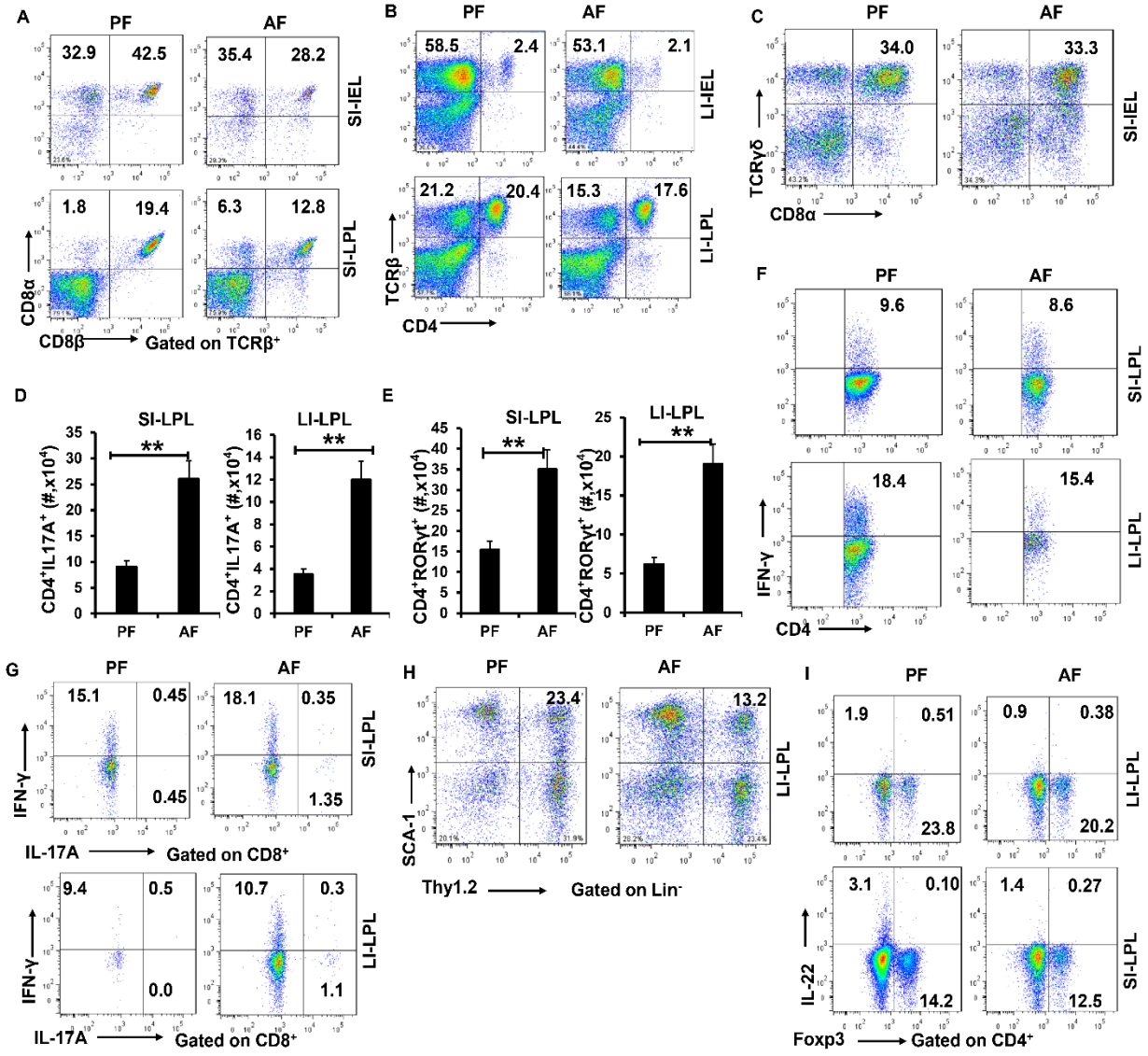

Figure S1 Increase of gut inflammation in ALD. WT mice were fed control (pair-fed, PF) or alcohol (alcohol-fed, AF) diet and sacrificed 15 - 22 days later.

(A-B) Representative flow cytometry plots and proportion of ($CD8\alpha^+CD8\beta^+$ $TCR\beta^+$) $CD8\alpha\beta^+$T cells, ($CD8\alpha^+CD8\beta^-$ $TCR\beta^+$) $CD8\alpha\alpha^+$T cells (A) and $CD4^+TCR\beta^+$ (B) among total $CD45^+$ IEL and LPL from large intestine (LI) and small intestine (SI) in PF and AF mice.

(C) Proportion of $CD8\alpha^{+}TCR\gamma\delta^{+}$ cells in SI-IEL populations.

(D-E) The number of $CD4^{+}$ $IL17A^{+}$ T cells (D) or $CD4^{+}ROR\gamma t^{+}$ T cells (E) from colon or small intestine LPL.

(F-G) Representative flow cytometry plots and proportion of $CD4^{+}IFN\text{-}\gamma^{+}$ (F) or IFN-γ and IL-17A (G) in $CD8\alpha^{+}$ T cells from colon or small intestine LPL.

(H) Proportion of $Lin^{-}Th1.2^{+}Sca\text{-}1^{+}$ ILCs in LI-LP populations.

(I) Intracellular staining of IL-22 and Foxp3 in $CD4^{+}$ T cells from colon or small intestine LPL.

Data in all panels are presented as Mean ± SEM and n=15 mice/group.

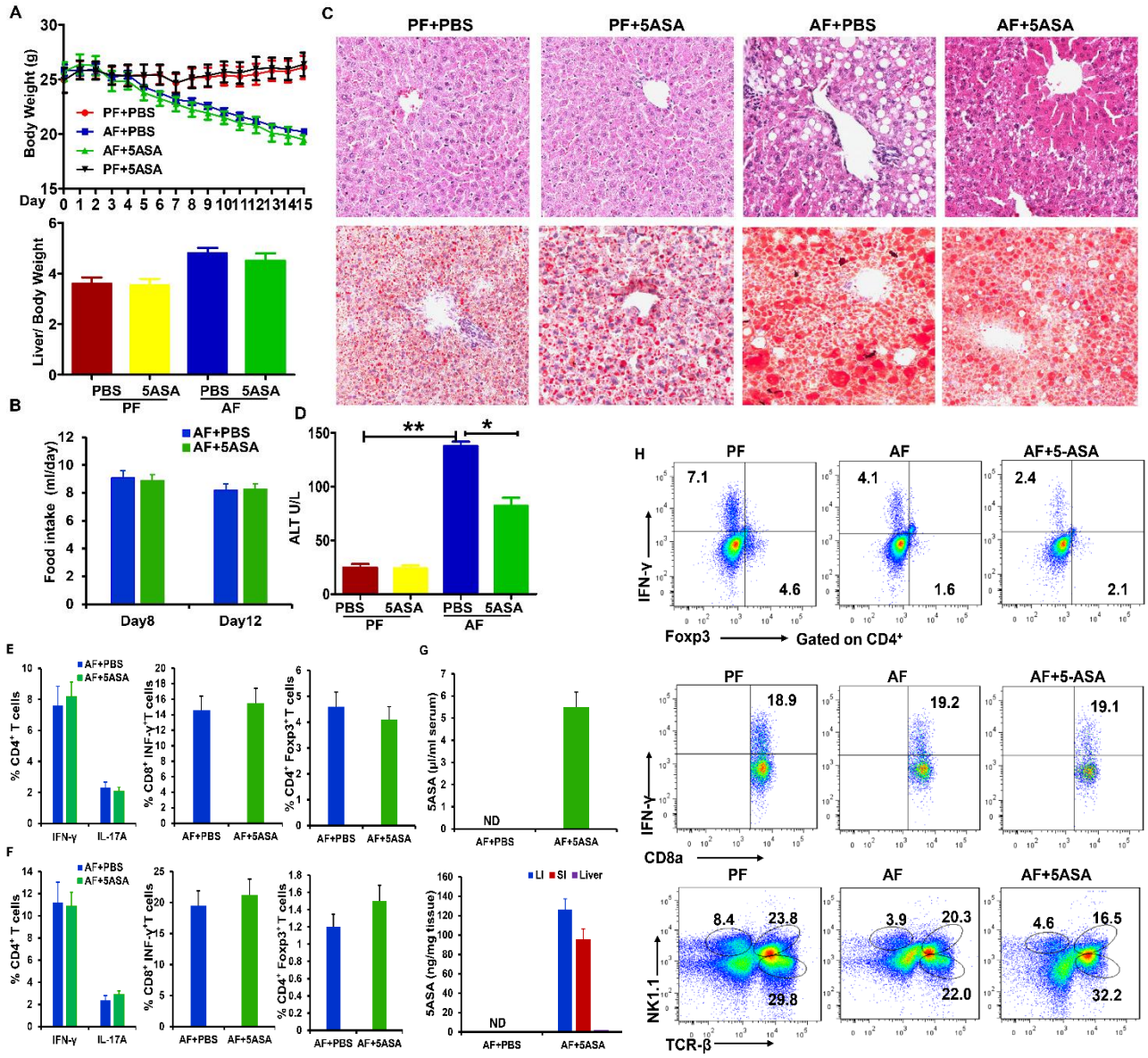
A
Body Weight (g)
PF+PBS
AF+PBS
AF+5ASA
PF+5ASA
Day
Liver/ Body Weight
PBS 5ASA PBS 5ASA
PF
AF
B
AF+PBS
AF+5ASA
Food intake (ml/day)
Day8
Day12
C
PF+PBS
PF+5ASA
AF+PBS
AF+5ASA
D
ALT U/L
**
*
PBS 5ASA PBS 5ASA
PF
AF
E
% CD4+ T cells
IFN-γ
IL-17A
% CD8+ INF-γ+T cells
% CD4+ Foxp3+T cells
AF+PBS
AF+5ASA
F
% CD4+ T cells
% CD8+ INF-γ+T cells
% CD4+ Foxp3+T cells
G
5ASA (μl/ml serum)
ND
5ASA (ng/mg tissue)
LI
SI
Liver
H
PF
AF
AF+5-ASA
IFN-γ
Foxp3
Gated on CD4+
7.1
4.6
4.1
1.6
2.4
2.1
CD8a
18.9
19.2
19.1
NK1.1
TCR-β
8.4
23.8
29.8
3.9
20.3
22.0
4.6
16.5
32.2

Figure S2 5-ASA improves liver inflammation in mice during alcohol feeding

(A-B) and (E-H). C57BL/6 mice on a pair-fed or chronic-binge ethanol diet, with 5-ASA oral supplementation (50 mg/kg/day) or vehicle for 15 days.

(A) Body weights of mice over time and the ratio of liver: body weight.

(B) Food intake.

(C-D) C57BL/6 mice were fed control or alcohol diet. At day 14, mice were started with 5-ASA oral supplementation (50 mg/kg/day) or PBS and sacrificed 2 weeks later. H&E and Oil red O staining of liver tissue (C); Serum levels of ALT (D).

(E) Proportions of Th1 T cells and Th17 T cells (left), IFNγ-producing $CD8^+$ T cells (middle), and $CD4^+Foxp3^+$ Tregs (right) in the spleens of mice.

(F) Proportions of Th1 T cells, and Th17 T cells (left), IFNγ-producing $CD8^+$ T cells (middle) and $CD4^+Foxp3^+$ Tregs (right) in the peripheral blood of mice.

(G) Concentrations of 5-ASA in serum (top), large, small intestine, or liver (bottom) as measured by HPLC ('ND' indicates non-detectable concentrations). n=5 mice/group.

(H) Intracellular staining of $CD4^+Foxp3^+$ and IFN-γ^+ T cells, $CD8^+$ IFN-γ^+ T cells and frequencies of NK cells, NKT cells and T cells in the liver.

Data in all panels are presented as Mean ± SEM and n=15 mice/group.

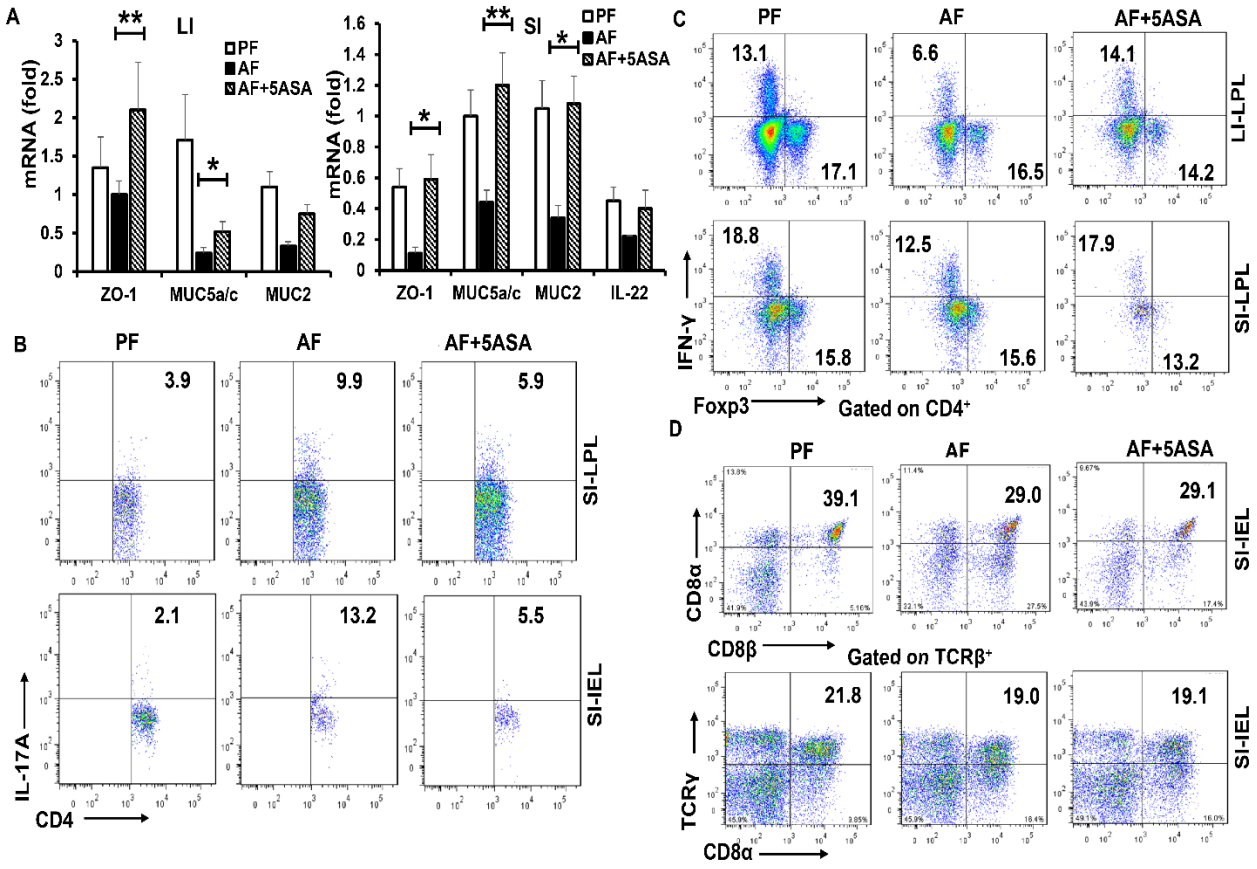

Figure S3 5-ASA improves gut inflammation in mice during alcohol feeding. C57BL/6 mice on a pair-fed or chronic-binge ethanol diet, with 5-ASA oral supplementation (50 mg/kg/day) or vehicle for 15 days.

(A) Real-time PCR analysis of the expression of indicated genes in the colon and small intestine.

(B) Intracellular staining of IL-17A in $CD4^+$ T cells in LPL and IEL of small intestine.

(C) Intracellular staining of $CD4^+Foxp3^+$ T cells and $CD4^+$ IFN-γ^+ T cells from LPL of colon and small intestine.

(D) Proportion of $CD8\alpha\beta^+TCR\beta^+$, $CD8\alpha\alpha^+TCR\beta^+$ or $CD8\alpha^+TCR\gamma\delta^+$ cells in the SI-IEL.

Data in all panels are presented as Mean ± SEM and n=15 mice/group.

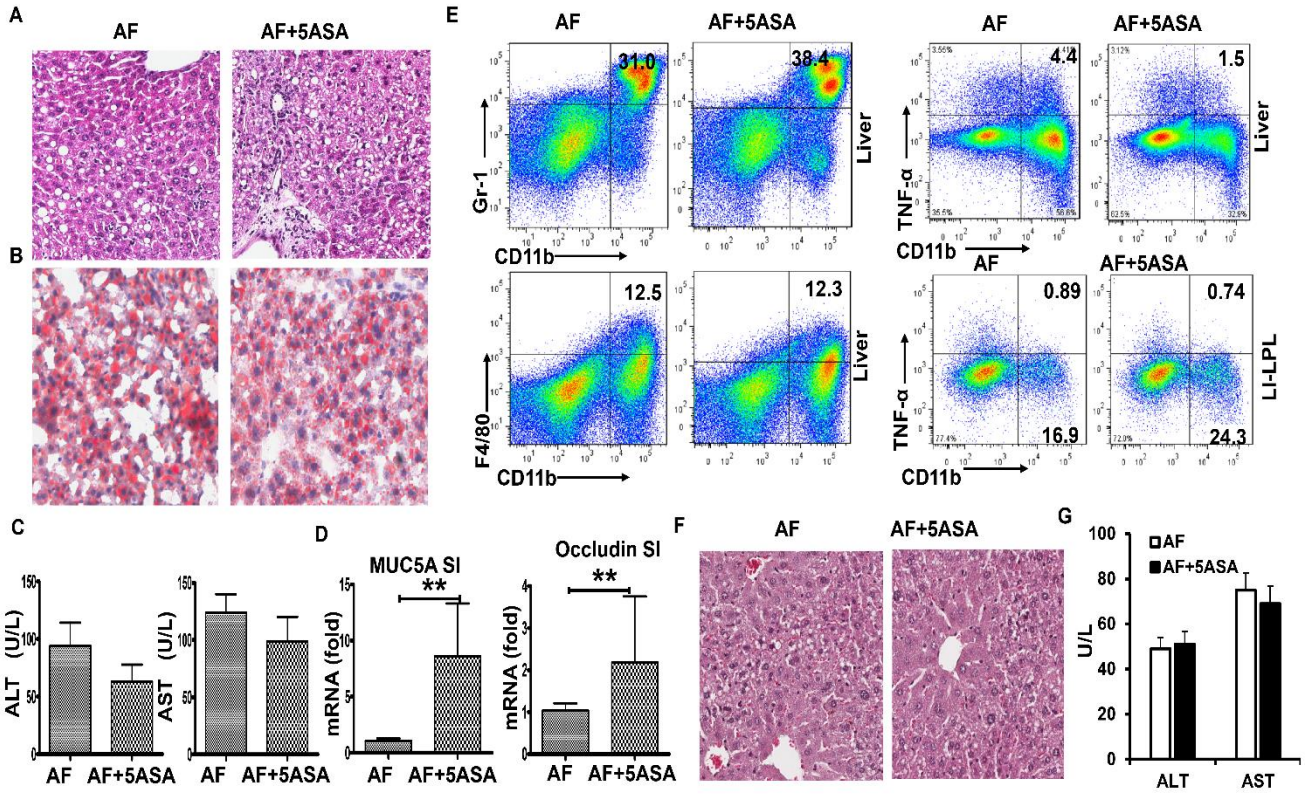

Figure S4 5-ASA targets Th17 cells-mediated adaptive gut immunity during alcohol feeding. Rag1$^{-/-}$ mice (A-G) or RORγt$^{-/-}$ (F-G) on chronic-binge ethanol diet, with 5-ASA oral supplementation (50 mg/kg/day) or vehicle for 15 days.

(A-B) H&E and Oil red O staining of liver tissue.

(C) Serum levels of ALT and AST.

(D) Real-time PCR analysis of the expression of indicated genes in the small intestine.

(E) Frequencies of immature myeloid cells (CD11b^{+}Gr-1^{+}), macrophages (CD11b^{+}F4/80^{+}), and TNF-producing myeloid cells in the liver and the LPL of colon of Rag1$^{-/-}$ mice.

(F) H&E staining of liver tissue in RORγt$^{-/-}$ mice.

(G) Serum levels of ALT and AST in RORγt$^{-/-}$ mice.

Data in all panels are presented as Mean ± SEM. n=7, ** P<0.01.

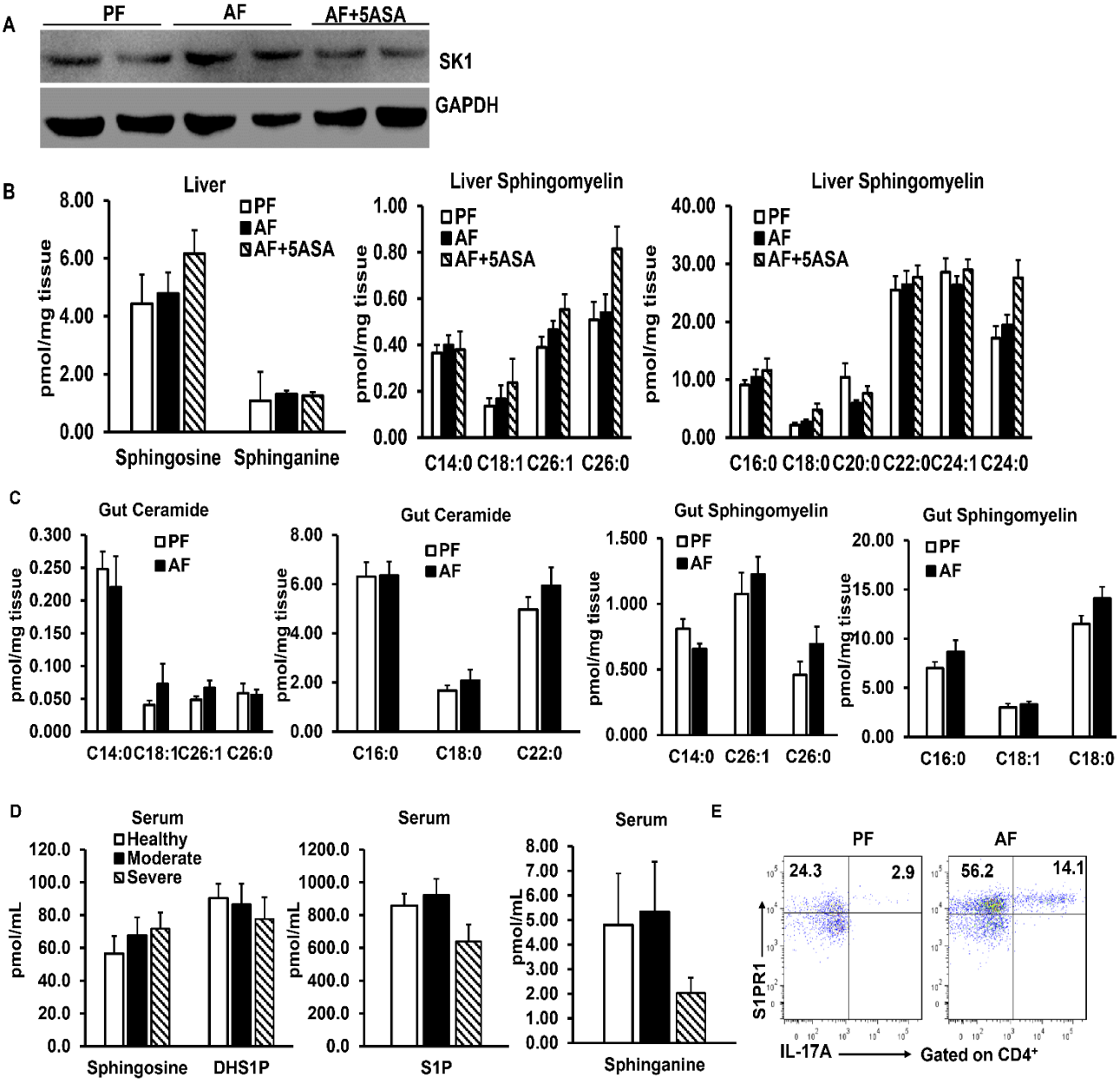

Figure S5 Activation of sphingosine kinase and S1P in ALD. C57BL/6 mice on a control or chronic-binge ethanol diet, with 5-ASA oral supplementation (50 mg/kg/day) or vehicle for 15 days.

(A) Western blot analysis of the expression of SK1 in the colon.

(B) Levels of Sphingosine, Sphinganine and Sphingomyelin in the liver.

(C) Levels of S1P, DHS1P, Ceramindes, Sphingomyelin in the gut.

(D) Levels of Sphingosine, DHS1P, S1P and Sphinganine in the serum of moderate, severe alcoholic hepatitis (AH) patients or healthy donors (normal liver). n=13

(E) Proportion of $CD4^+$ $S1PR1^+$ in the SI-LPL.

Data from mice are presented as Mean ± SEM. n=8.

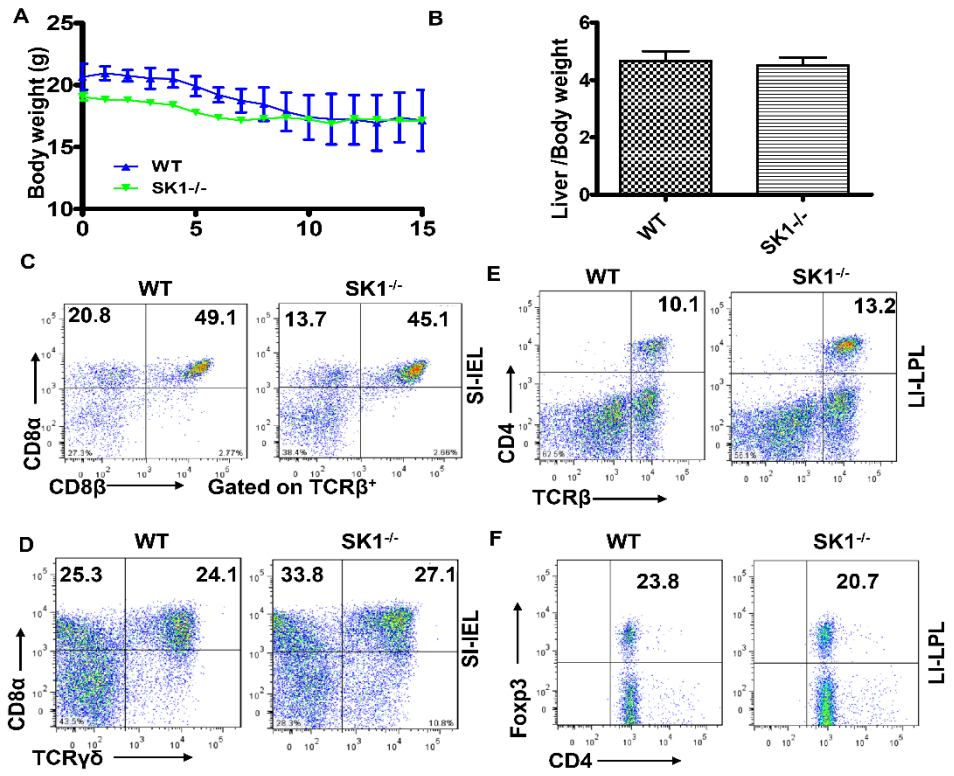

Figure S6 Deficiency of SK1 attenuates alcoholic liver inflammation, steatosis, and damage. WT or SK1$^{-/-}$ mice were fed alcohol diet and sacrificed 15 days later.

(A) Body weights of mice over time.

(B) The ratio of liver: body weight.

(C-F) Proportion of CD8αβ^{+}TCRβ^{+}, CD8αα^{+}TCRβ^{+}(C) and CD8α^{+}TCRγδ^{+} (D) in the SI-IEL; and CD4^{+}TCRβ^{+} (E), CD4^{+}Foxp3^{+} (F) in the LI-LPL.

Data in all panels are presented as Mean ± SEM. n=7.

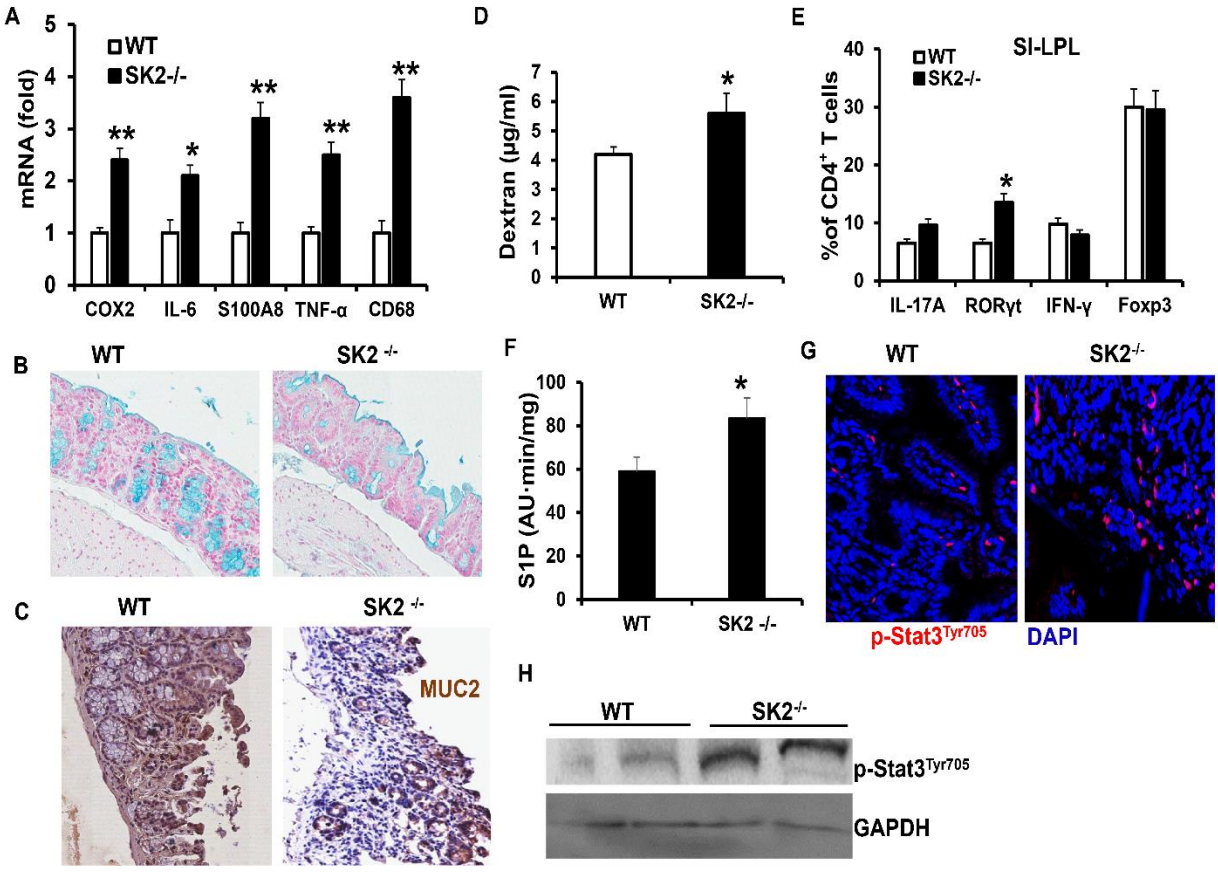

Figure S7 Deficiency of SK2 promotes liver and gut inflammation and induces the accumulation of gut Th17 cells in ALD. WT or SK2$^{-/-}$ mice on a chronic-binge ethanol diet, with/without 5-ASA oral supplementation (50 mg/kg/day) or vehicle for 15 days.

(A) Real-time PCR analysis of the expression of indicated genes in the liver.

(B) Alcian Blue stained images of colonic tissue.

(C) Immunohistochemistry staining of mucin 2 in the colon.

(D) Plasma levels of Dextran-FITC for gut permeability;

(E) Intracellular staining of IL-17A, IFN-γ, Foxp3 or RoRγt in $CD4^+$ T cells from small intestine LPL.

(F) Relative levels of S1P in the ileum of alcohol-fed mice.

(G-H) Immunofluorescence (G) or Western blotting (H) was used to evaluate the expression of pSTAT3 in the ileum.

Data in all panels are presented as Mean ± SEM. n=7 * P<0.05; ** P<0.01

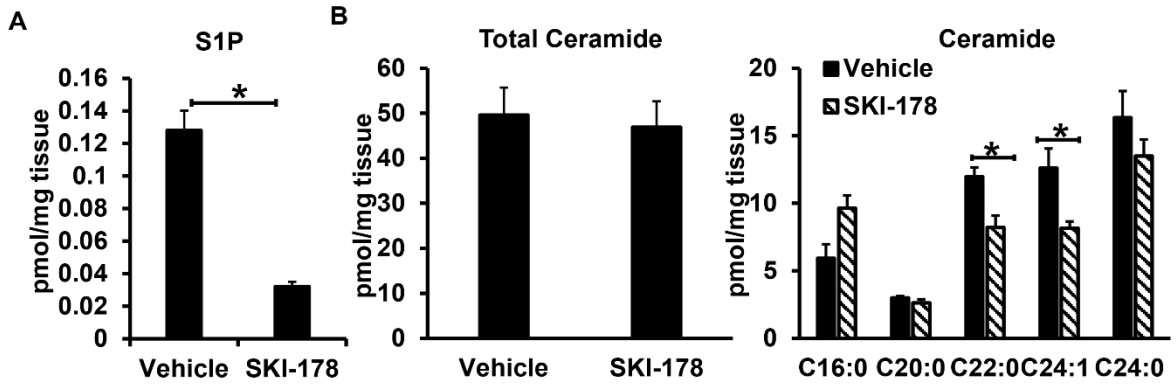

Figure S8 Pharmacologic intervention via inhibition of S1P/SPR1 signaling ameliorates ALD progression. WT mice were fed an alcohol diet, treated with SK1-I (5 mg/kg, i.v every two days) with/without 5-ASA (50mg/kg, orally given every day) and sacrificed 15 days later.

(A) Relative levels of S1P in the liver of alcohol-fed mice with/without SKI-178 treatment.

(B) Levels of ceramides in the liver with/without SKI-178 treatment.

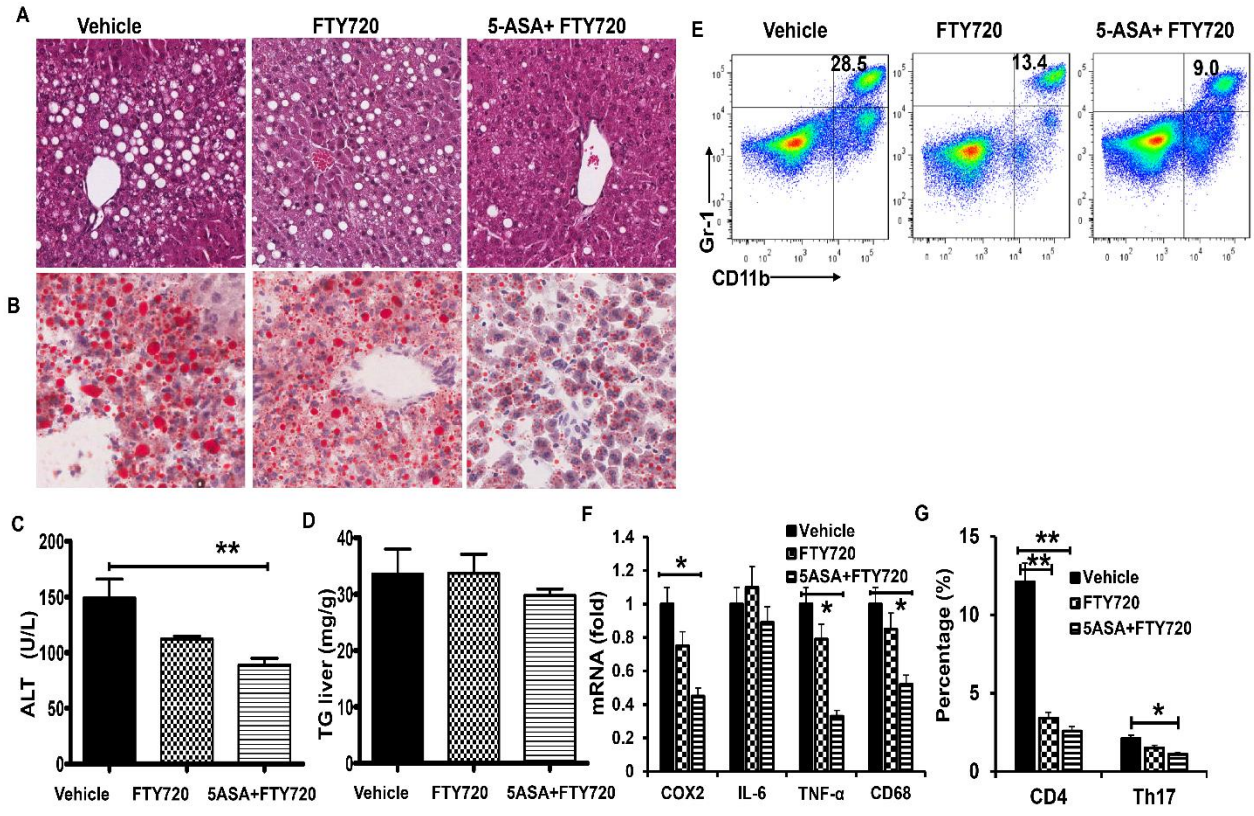

Figure S9 Pharmacologic intervention via inhibition of S1P/SPR1 signaling ameliorates ALD progression. WT mice were fed an alcohol diet, treated with FTY720 (1mg/kg, orally given every day) with/without 5-ASA (50mg/kg, orally given every day) and sacrificed 22 days later.

(A) Liver injury was assessed by liver H&E staining.

(B) Steatosis was evaluated by Oil-red-O staining.

(C) Serum ALT levels.

(D) Hepatic triglycerides levels.

(E) Frequencies of immature myeloid cells ($CD11b^{+}Gr\text{-}1^{+}$) in the liver.

(F) Real-time PCR analysis of the expression of indicated genes in the liver.

(G) The proportion of $CD4^{+}$ cells or Th17 cells in the liver.

Data in all panels are presented as Mean ± SEM. n=7 * P<0.05; ** P<0.01